

CT and MRI findings in focal eosinophilic infiltration of the liver

Bao-liang Guo,¹ Qiu-gen Hu,¹ Fu-sheng Ouyang,¹ Bin Zhang,^{2,3} Yu-hao Dong,⁴ Xiao-ning Luo,⁴ Zhou-yang Lian,⁴ Shui-xing Zhang^{2,3}

¹Department of Radiology, The First People's Hospital of Shunde, Foshan, Guangdong, People's Republic of China

²Medical Imaging Center, First Affiliated Hospital of Jinan University, Guangzhou, People's Republic of China

³Institute of Molecular and Functional Imaging, Jinan University, Guangzhou, People's Republic of China

⁴Department of Radiology, Guangdong General Hospital/Guangdong Academy of Medical Sciences, Guangzhou, People's Republic of China

Abstract

Objectives: To investigate the findings of computed tomography (CT) and magnetic resonance imaging (MRI) of focal eosinophilic infiltration (FEI) of the liver.

Methods: A retrospective study including 29 patients with confirmed FEI of the liver was performed. We evaluated the lesions' number, distribution, size, shape, margin, attenuation or signal intensity characteristics, the enhancement pattern, and some special features. Spearman correlation analysis was used to analyze the correlation between the number of lesions and the eosinophil counts in peripheral blood.

Results: In all, 108 lesions were detected in 29 cases, including two cases with single lesion and the remaining 27 cases with multiple lesions. The mean size of all lesions was 34 mm (range, from 3 to 61 mm). 95 (88%) lesions were located in subcapsular parenchyma or surrounding the portal vein. Most (66%) subcapsular lesions were wedge shaped and all lesions surrounding portal vein were round shaped. However, the hepatic parenchymal lesions were irregular or round shaped. All lesions showed ill-defined margins. On pre-contrast CT images, the lesions showed slightly low attenuation or iso-attenuating. On T1-weighted and T2-weighted images, the lesions were slightly iso-/hypointense and hyperintense, respectively. A total of 23 (79.3%) cases were gradually enhanced. Branches of portal vein went through the lesions in all cases; 12 had 'stripe sign' and 16 had 'halo ring sign.' Spearman analysis indicated a

significant correlation between the number of lesions and the increased eosinophils in peripheral blood ($r = 0.627$, $p = 0.0003$).

Conclusions: Special CT and MRI features and increased eosinophils may strongly suggest the diagnosis of FEI of the liver.

Key words: Eosinophilia—Hepatic infiltration—Computed tomography—Magnetic resonance imaging

It is accepted that hypereosinophilia may be associated with tissue damage. All organ systems may be susceptible to the effects of sustained eosinophilia. The common organ systems are hematologic (100%), cardiovascular (58%), utaneous (56%), neurologic (54%), pulmonary (49%), and gastrointestinal (38%) systems [1]. Liver is involved in only 20%–30% of patients [2]. Eosinophilic infiltration into the liver (mainly into the periportal space) is an uncommon entity that is characterized by multiple focal lesions. The resultant focal lesion is an abscess or granuloma with marked eosinophilic infiltrates on pathology, also called eosinophilic abscess or eosinophilic granuloma. Although the mechanism of eosinophil-related tissue damage is poorly understood, the process might involve the infiltration of eosinophils into tissue damage related to eosinophil function and products (e.g., eosinophil major basic protein and eosinophil cationic protein), and the occurrence of thromboembolic phenomena [3]. Eosinophilic organ infiltration has been described secondary to identifiable causes such as drug hypersensitivity, allergic diseases, malignancies, hypereosinophilic syndrome, collagen vascular diseases, and,

Bao-liang Guo and Qiu-gen Hu contributed equally to this work.

Correspondence to: Zhou-yang Lian; email: immortalotus@163.com; Shui-xing Zhang; email: shui7515@126.com

most commonly, to parasitic infections [4, 5]. Some researches have revealed pathologic changes in various organs such as heart, lung, and brain caused by eosinophilia [6–9]. Most radiologic reports regarding eosinophilia have focused on pulmonary changes.

Some previous reports have described some specific radiologic findings of FEI of the liver on ultrasound (US) and computed tomography (CT) images. However, few studies describe magnetic resonance imaging (MRI) features [10–12]. Compared with CT, MR provides better soft tissue contrast resolution and thus can distinguish enhancing focal lesions from hepatic tissue based on differences in the lesion-to-liver contrast enhancement during both the equilibrium and portal venous phases [13]. Diffusion-weighted imaging (DWI) has become a practical tool for the detection and the characterization of hepatic lesions. Malignant liver tumors usually have lower apparent diffusion coefficients (ADCs) than benign liver tumors. Thus, combined imaging modalities are superior to single modality in evaluating this disease.

Generally, it is not easy to discriminate FEI from other lesions in patients with underlying malignancies by radiologic findings alone [14]. Several identifying radiologic features of FEI also appear in other diseases, particularly with hepatic metastases. Therefore, the diagnosis of eosinophilic infiltration in the liver is of importance radiologically and clinically.

The most important clinical feature of eosinophilic infiltration is the range of eosinophils in the peripheral blood, for which the upper limit of normal is 3%–5%, with a corresponding absolute eosinophil count of 350–500/mm³ [15]. Hypereosinophilia has generally been defined as a peripheral blood eosinophil count greater than 1500/mm³ and may be associated with tissue damage [1]. However, few reports focused on the imaging features caused by hypereosinophilia.

Because appropriated surgical treatment might otherwise not be undertaken, the preoperative diagnosis of hepatic eosinophilic infiltration presenting as hepatic nodules is important. Moreover, it occurs with a higher incidence among patients with an underlying malignancy. To our best of knowledge, there is no study described joint CT and MRI features of hepatic FEI and uncovered the association between the number of hepatic FEI and the increase of eosinophils in peripheral blood.

Accordingly, the purpose of this study was to find some specific CT and MRI findings in 29 patients with confirmed FEI of the liver and thus improve the radiologists' diagnostic ability of this disease.

Materials and methods

Patients

This retrospective study was approved by our Institutional Review Board, and informed consent was waived for the review of clinical records and radiologic images.

We retrospectively reviewed and collected the medical records from the radiology department between January 2005 and June 2015. A total of 237 patients had been diagnosed with hypereosinophilia by laboratory examination and bone marrow biopsy. Of these, 29 patients with a confirmed hepatic eosinophilic infiltration were enrolled in this study. The diagnosis of all patients was based on percutaneous needle biopsy.

All patients underwent contrast-enhanced upper abdominal CT and/or MRI scan pre-treatment. The initial imaging detecting the hepatic eosinophilic infiltration was by a helical triple-phase enhanced CT scan ($n = 24$), and a triple-phase enhanced MRI scan ($n = 2$), of which, three cases underwent CT and MRI scan at the same time.

CT protocol

All the triphasic dynamic helical CT scanings were performed on Lightspeed Ultra (GE Medical Systems, Milwaukee, WI) with a bolus injection of 90 mL of nonionic contrast media (Iopromide 370; Schering AG, Berlin, Germany) via the antecubital vein at a rate of 4–5 mL/s by power injector, with images obtained 36–44, 70–78, and 180 s after the start of contrast injection during the hepatic arterial, portal, and equilibrium phase, respectively. The parameters were as follows: detector configuration = $64 \times 0.625 \text{ mm}^2$, slice thickness = 3 mm, reconstruction interval = 2 mm, table speed = 46.9 mm/rotation, rotation time = 0.5–0.75 s, tube current = 250 mAs, tube voltage = 120 kVp, matrix = 512×512 .

MRI protocol

MR imaging was performed on 5 patients with a 1.5 T (Signa Horizon; GE Medical Systems, Milwaukee, WI) MRI unit. All images were obtained in the transverse plane using a four-channel phased-array body coil. Baseline MR sequences included a breath-hold T1-weighted, spoiled gradient recalled echo (GRE) sequence; a respiratory-triggered, T2-weighted, rapid acquisition relaxation-enhanced (RARE) sequence; and a single-shot fast spin-echo (SSFSE) sequence. The T2-weighted RARE imaging was performed using the parameters: TR/TE = 3000–7500/97.1 ms; echo-train length = 12; matrix = 512×384 ; chemical shift fat suppression; array spatial sensitivity encoding technique (ASSET); acceleration factor of 2; and a signal average of 3. T2-weighted, SSFSE imaging was performed using the parameters: TR/TE = infinite/86.9 ms; flip angle = 90°; echo-train length = 240; and matrix = 384×192 . Breath-hold T1-weighted, spoiled GRE (in-phase and out-of-phase) sequence was performed with the parameters: TR/TE = 140/2.4 and 5.8 ms; flip angle = 70°; matrix = 512×192 ; and a

Imaging findings

A total of 108 lesions of eosinophilic infiltration were detected in 29 cases. Of the 29 cases, 2 were with single lesion and the remaining 27 were with multiple lesions (1–4 lesions per case). The mean size of all lesions was 34 mm (range, from 3 to 61 mm). A total of 101 (93.5%) lesions were located in subcapsular parenchyma or surrounding the portal vein. Most (66%) subcapsular lesions were wedge shaped, and all lesions surrounding portal vein were round shaped. However, the hepatic

parenchymal lesions were irregular or round shaped (Table 1). Table 2 shows the appearances of pre-contrast and contrast-enhanced CT and MRI images.

CT findings

All lesions were hypo-attenuating or iso-attenuating with ill-defined margins on pre-contrast CT images. Only 65 (64%) were detected on pre-contrast CT images. On arterial phase images, only 36 (36%) lesions with low or high attenuation were found and the 65 (64%) lesions showed iso-attenuation that could not be seen. On portal phase images, 101 lesions were detected, 90 (89%) of which showed low attenuation with well-defined margins, 4 (4%) showed high attenuation and 7 (7%) showed iso-attenuation. Special features including branches of portal vein went through the lesions; ‘stripe sign’ and ‘halo ring sign’ were observed (Figs. 2, 3). On equilibrium phase images, 86 (80%) lesions showed iso-attenuation or nearly iso-attenuation. The detection rates of CT scanning were 64%, 36%, 93%, and 20% on pre-contrast images, arterial, portal, and equilibrium phases,

Table 1. The summary of lesion shape and location

	Surrounding the portal vein	Subcapsular	Hepatic parenchymal
Wedge shape	13 (25%)	28 (65.1%)	0
Round shape	32 (61.5%)	3 (7.0%)	5 (38.5%)
Irregular shape	7 (13.5%)	12 (27.9%)	8 (61.5%)
Total	52 (48.1%)	43 (39.8%)	13 (12.0%)

Except where otherwise indicated, values are the number of lesions (percentage)

Irregular shape was defined as random shape

Table 2. The appearances of pre-contrast and contrast-enhanced CT and MRI images

	Pre-contrast			Arterial phase			Portal phase			Equilibrium phase		
	Hypo	Iso	Hyper	Hypo	Iso	Hyper	Hypo	Iso	Hyper	Hypo	Iso	Hyper
CT (<i>n</i> = 101)	65 (64%)	36 (36%)	0	28 (28%)	65 (64%)	8 (8%)	90 (89%)	7 (7%)	4 (4%)	15 (15%)	81 (80%)	5 (5%)
MRI (<i>n</i> = 21)												
T ₁ WI	9 (43%)	12 (57%)	0	2 (10%)	17 (81%)	2 (10%)	18 (86%)	1 (5%)	2 (10%)	1 (5%)	17 (81%)	3 (14%)
T ₂ WI	0	4 (19%)	17 (81%)	–	–	–	–	–	–	–	–	–

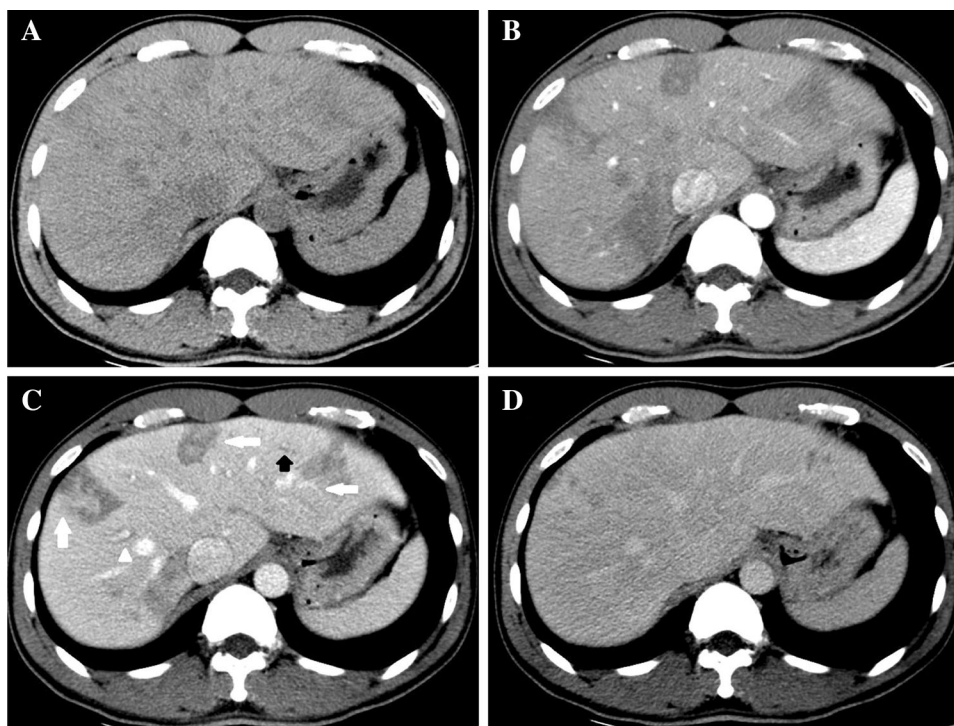


Fig. 2. A 43-year-old man with hypereosinophilic syndrome. **A** The pre-contrast CT image shows multiple isodense lesions in subcapsular parenchyma or surrounding the portal vein. **B** The lesions are slightly hypo-attenuating or iso-attenuating relative to the liver in the arterial phase. **C** In the portal phase, the lesions became clear and hypo-attenuating relative to the liver. *White arrow* shows branches of portal vein through the lesions, *white arrowhead* shows ‘stripe sign’ accompanied the portal vein branches, *black arrow* shows ‘halo ring sign’ around the portal vein. **D** In the equilibrium phase, lesions show iso-attenuating.

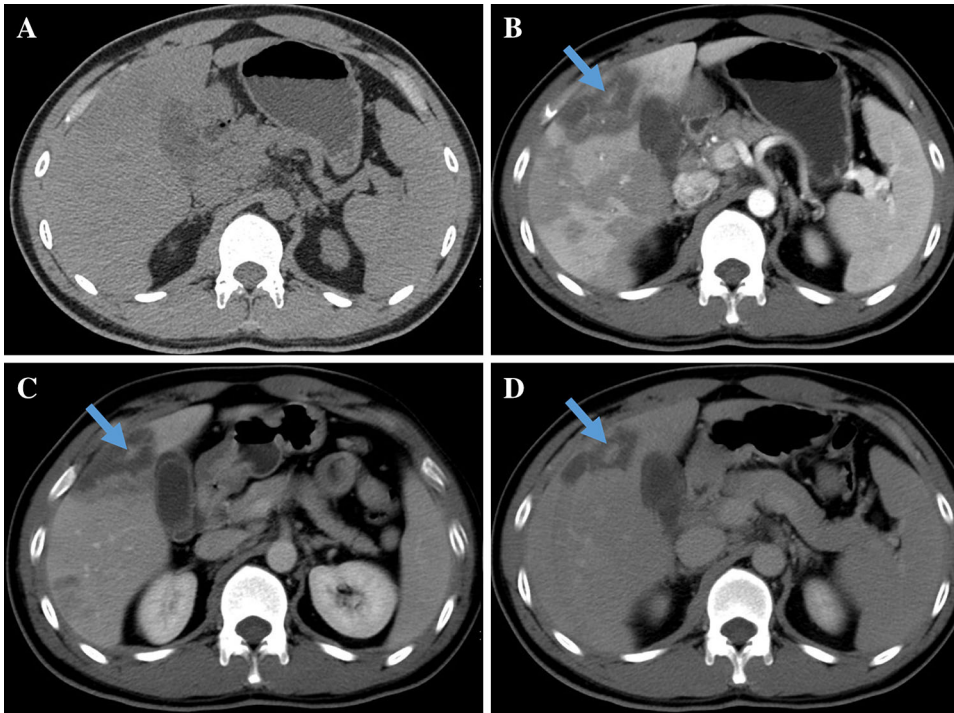


Fig. 3. A 33-year-old man with hypereosinophilic syndrome and numerous eosinophilic infiltrations at 68% serum eosinophils ($16.45 \times 10^9/L$). **A** Pre-contrast scan shows slightly low attenuated lesions with ill-defined margins. **B–D** On arterial, portal, and equilibrium phases, the lesion shows prominent low attenuation in contrast to the adjacent liver with size reduction. We could observe branches of portal vein went through the lesion (blue arrow).

respectively. The detection rates of pre-contrast images and postcontrast images were significantly different ($p < 0.012$, for all).

MRI findings

MR images showed 21 lesions of FEI in 5 patients. On T1-weighted images, 12 (57%) lesions were isointense and 9 (43%) were hypointense. On T2-weighted images, 17 (81%) lesions were hyperintense and 4 (19%) lesions were isointense. All lesions were with poorly defined margins. After Gd-DTPA injection, 17 (81%) lesions were isointense relative to the liver on the arterial phase. On the portal phase, 18 (86%) lesions became hypointense relative to the liver. On the equilibrium phase, 17 (81%) lesions were isointense or nearly isointense, only 1 (5%) lesion showed hypointense and 3 (14%) lesions showed hyperintense. One case showed mixed hypointensity in the hepatobiliary phase (Fig. 5). All cases showed hyperintensity in both low and high b value ranges on DWI, with ADCs of less than $1.00 \times 10^{-3} \text{ mm}^2/\text{s}$ (Fig. 5). Special features including branches of portal vein went through the lesions, and ‘stripe sign’ were observed (Figs. 4, 5). The detection rates of MR scanning were 81%, 20%, 96%, and 19% in pre-contrast images, the arterial, portal, and equilibrium phases, respectively. The detection rate of lesions in portal phase images was the highest ($p < 0.001$ for each comparison).

A total of 14 lesions were detected in 3 patients underwent both. For CT, there were 8 (57.1%), 5 (35.7%), 13 (92.9%), and 3 (21.4%) lesions detected on pre-contrast, arterial phase, portal phase, and equilib-

rium phase images, respectively, whereas for MRI, there were 11 (78.6%), 3 (21.4%), 14 (100%), and 3 (21.4%) lesions detected on pre-contrast, arterial phase, portal phase, and equilibrium phase images, respectively.

Table 3 shows the enhancement pattern and special signs on dynamic contrast-enhanced images, and 23 (79.3%) cases were gradually enhanced. Branches of portal vein went through the lesions were found in 29 cases; 12 found hypodense or hypointense ‘stripe sign’ accompanying with the portal vein branches, and 16 found low attenuating or hypointense ‘halo ring’ around the portal vein.

The interrater reliability between two readers in terms of imaging features was assessed using simple Kappa coefficient, ranging from 0.87 to 1.00.

Discussion

Several reports have described CT or MR findings of eosinophilic liver diseases, including eosinophilic infiltration and eosinophilic abscesses [10, 17, 18]. In this study, we retrospectively analyzed the CT and MRI findings of hepatic eosinophilic infiltration and identified some specific features that are helpful in differentiating it from the other liver diseases, especially metastatic tumor. In addition, spearman correlation analysis indicated a strong correlation between the number of lesions and the increased eosinophils in peripheral blood ($r = 0.627$, $p = 0.0003$), which was consistent with the previous studies [16].

By analyzing the 108 lesions in 29 patients, we found that most (88.6%) lesions were located in subcapsular

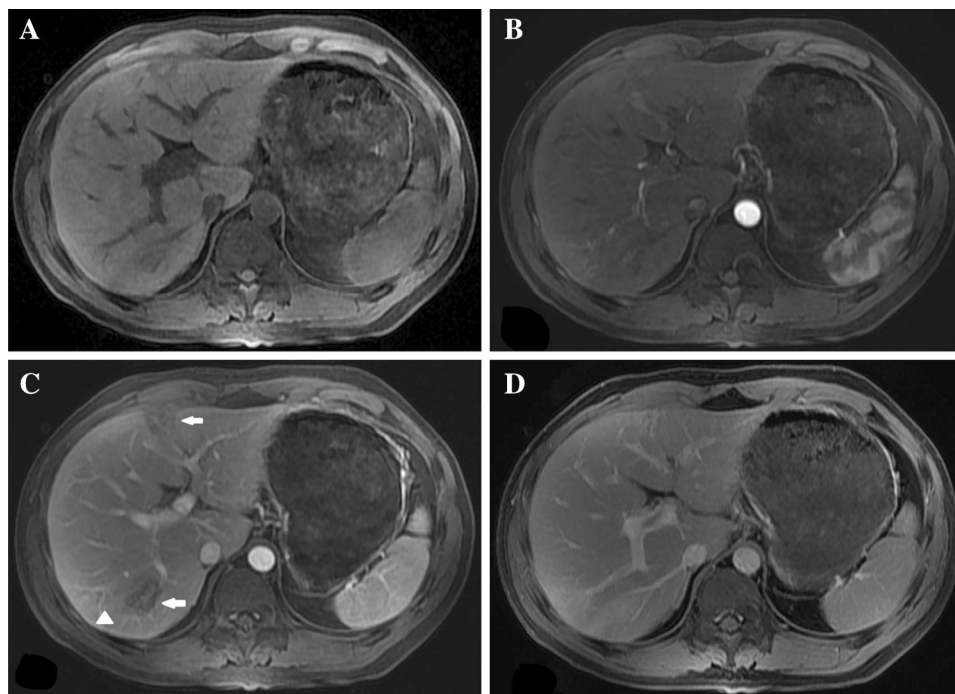


Fig. 4. A 42-year-old with hypereosinophilic syndrome. **A** The unenhanced T1-weighted image shows multiple isointense lesions in subcapsular parenchyma or surrounding the portal vein. **B** The lesions are isointense relative to the liver in the arterial phase. **C** During the portal phase, the

lesions became hypointense relative to the liver. *White arrow* shows branches of portal vein went through the lesions, *white arrowhead* shows 'stripe sign' accompanied with the portal vein branches. **D** Lesions show isointense on the equilibrium phase.

parenchyma or surrounding the portal vein. For subcapsular lesions, wedge shape was seen in most cases. All lesions surrounding portal vein were round shaped. However, the hepatic parenchymal lesions were irregular or round shaped. These findings support the view that the lesions located around portal area and peripheral vascular [19, 20].

On pre-contrast and unenhanced T1-weighted images, about 20%–60% lesions are iso-attenuated or isointense, which are likely to be missed during the diagnosis, but most of them were hyperintense on T2-weighted images [21]. Regarding the enhancement pattern of the dynamic study, it should be noted that the lesions appeared poorly defined low attenuating or hypointensity during the portal phase, which was regarded as a main imaging finding of FEI [14]. In this present study, 23 (79.3%) cases appeared as iso-attenuating or isointense on arterial phase, poorly defined low attenuating or hypointense on portal phase, and iso-attenuating or isointense on equilibrium phase, that is, 'iso-hypo-iso' enhancement pattern. Thus, one of the characteristic imaging findings of hepatic eosinophilic infiltration is reported to be most conspicuous during the portal phase and to gradually become obscured during the equilibrium phase in CT scan. However, the dynamic-enhanced MRI of hepatic FEI is somewhat variable according to

the previous reports. A study found that the lesions (60%) presented nodular or rim or perilesional enhancement during the arterial phase [22]. Sun et al. observed that eosinophilic infiltration was hyperintense on the portal phase (82%) and equilibrium phase (77%) after the injection of Gd-DTPA [13]. Kim et al. [11] reported that 50% of focal eosinophilic liver diseases were isointense during the portal phase. Our results showed that most focal lesions showed hypointensity on the portal (86%) and equilibrium phase (5%) in relation to the surrounding liver parenchyma after a bolus injection of contrast [11]. It indicated that portal phase was the optimal phase to detect the FEI [23]. All lesions in our study showed hyperintensity in both low and high b values on DWI, which means that water molecules were being restricted within the lesions. However, the results suggest that DWIs with ADCs on lesions might demonstrate malignant features. Therefore, DWIs and ADCs are not likely to be helpful in differentiating FEIs from other malignant tumors, such as liver metastases.

The other important findings in terms of enhancement pattern were as follows: (1) most lesions (79.3%) showed continuous homogenous enhancement pattern during the dynamic study; (2) in all cases, branches of portal vein went through the lesions; (3) 12 cases were found low attenuating or hypointense 'stripe sign'

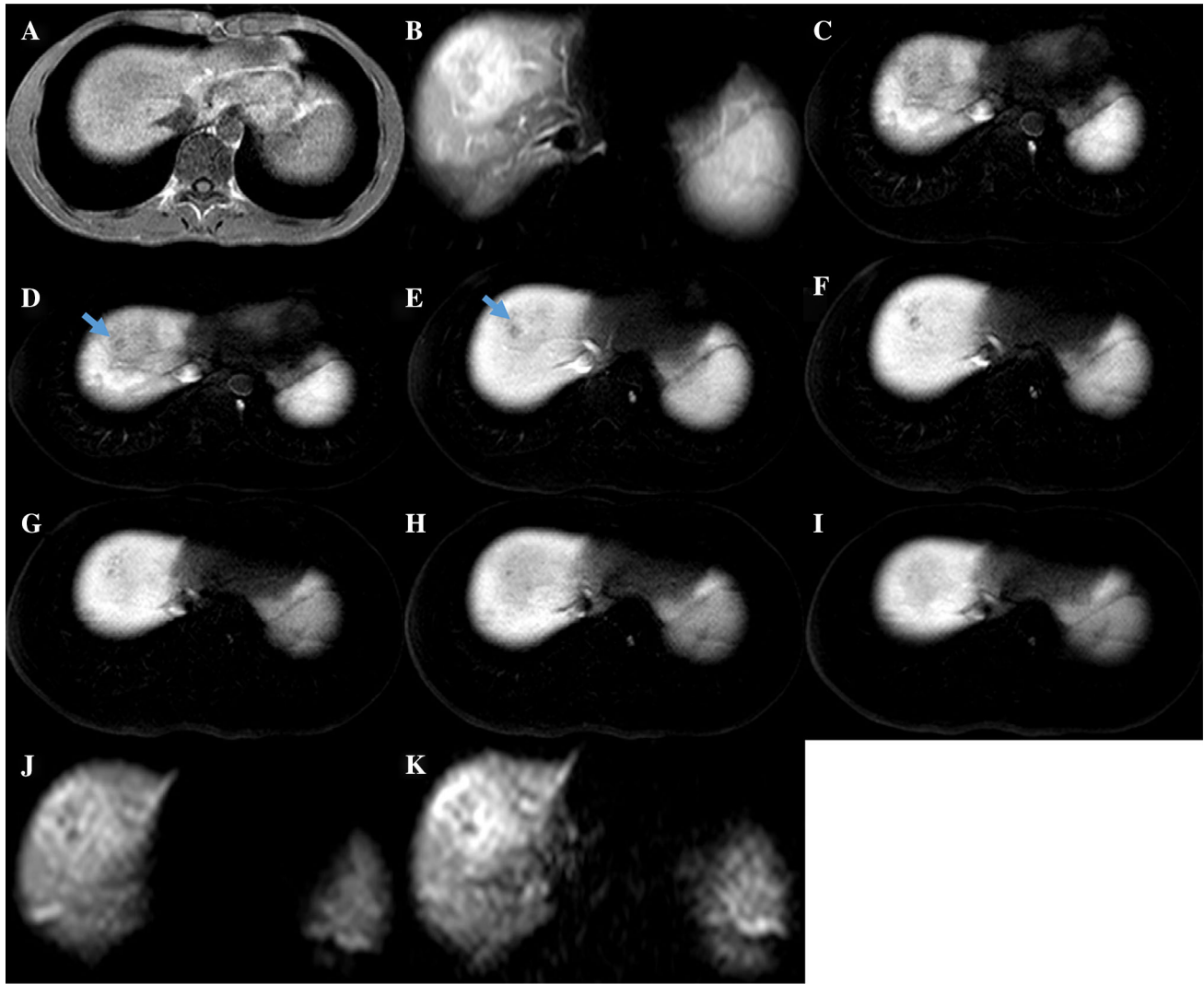


Fig. 5. A 31-year-old man with hypereosinophilic syndrome and numerous eosinophilic infiltrations at 72% serum eosinophils ($16.29 \times 10^9/L$). **A** On T1-weighted image, the lesion shows iso-/hypointensity relative to the liver. **B** On T2-weighted image, the lesion shows mixed hyperintensity. **C** On arterial phase, the lesion shows slight enhancement and hypo-intensity relative to the liver. **D–E** On portal and equi-

librium phases, we could observe ‘halo ring sign’ (blue arrow). **F–I** On hepatobiliary phase (3, 10, 15, 20, and 30 min after the contrast injection), the lesion shows mixed hypointensity with size reduction. **J, K** On DWI, the lesion shows hyperintensity in both low and high b value ranges, with the corresponding ADC of less than $1.00 \times 10^{-3} \text{ mm}^2/\text{s}$.

Table 3. The enhancement pattern and special signs

Characteristics	Descriptions	n (%)
Iso-hypo-iso pattern	Lesions showed iso-attenuation or isointensity to the liver on arterial phase, low attenuation/hypointensity on portal phase, and iso-attenuation/isointensity on equilibrium phase	23 (79.3%)
Branches of portal vein went through the lesion	Branches of portal vein went through the lesion and the shape and size of it did not be influenced by the lesion	29 (100%)
‘Stripe sign’	Low attenuating or hypointense lesions accompanying with the branches of portal vein, which like “stripe”	12 (41.4%)
‘Halo ring sign’	Low attenuating/hypointense lesions located around the portal vein, like “halo ring”	16 (55.2%)

accompanying with the portal vein branches; (4) and 16 cases were found low attenuating or hypointense ‘halo ring sign’ around the portal vein. The exact mechanisms for ‘stripe sign’ and ‘halo ring sign’ remain unclear. These findings had not been reported by the previous studies and were helpful to differentiate FEI from other liver diseases, such as metastasis. However, in patients with malignancy, it is difficult to exclude metastasis based only on radiologic images. Histologic confirmation is advised despite the presence of metastasis.

Our study also had some limitations. First, although we used 18-gauge automated biopsy guns, the specimens were too small to provide an exact pathologic correlation with the imaging findings. Second, various patterns in the dynamic studies depended on a variety of conditions, such as stage, age, and severity of eosinophilic infiltration. Lastly, fibrous stroma in the focal lesion might play a role in contrast enhancement in an equilibrium phase scan. Despite some fibrous stroma in our pathology specimen, it is difficult to explain the definite relation between MR findings and pathology in patients.

In summary, CT and MR imagings play the important role in the detection and characterization of focal eosinophilic infiltrations of the liver. Subcapsular location, obscure margins, continuous homogenous enhancement, branches of portal vein through the lesions, ‘halo ring sign,’ ‘stripe sign,’ and hypereosinophilia could be characteristic features of FEI of the liver. These results concerning the diagnosis of this disease may be useful in daily practice.

Acknowledgments This study was supported by Grants from The National Scientific Foundation of China (81571664), The Science and Technology Planning Project of Guangdong Province, (2014A020212244, 2016A020216020), The Commission on Innovation and Technology of Guangdong Province (201605110912158), and The Clinical Research Foundation of Guangdong General Hospital (2015zh04).

References

1. Gotlib J (2015) World Health Organization-defined eosinophilic disorders: 2015 update on diagnosis, risk stratification, and management. *Am J Hematol* 90(11):1077–1089
2. Yan BM, Shaffer EA (2009) Primary eosinophilic disorders of the gastrointestinal tract. *Gut* 58(5):721–732
3. Fauci AS, Harley JB, Roberts WC, et al. (1982) NIH conference. The idiopathic hypereosinophilic syndrome. Clinical, pathophysiologic, and therapeutic considerations. *Ann Intern Med* 97(1):78–92
4. Cottin V, Bel E, Bottero P, et al. (2017) Revisiting the systemic vasculitis in eosinophilic granulomatosis with polyangiitis (Churg-Strauss): a study of 157 patients by the Groupe d'Etudes et de Recherche sur les Maladies Orphelines Pulmonaires and the European Respiratory Society Taskforce on eosinophilic granulomatosis with polyangiitis (Churg-Strauss). *Autoimmun Rev* 16(1):1–9
5. Lee T, Lee YS, Yoon SY, et al. (2012) Clinical characteristics that distinguish eosinophilic organ infiltration from metastatic nodule development in cancer patients with eosinophilia. *World J Surg Oncol* 10:175
6. Simon D, Wardlaw A, Rothenberg ME (2010) Organ-specific eosinophilic disorders of the skin, lung, and gastrointestinal tract. *J Allergy Clin Immunol*, 126(1):3–13, 14–15.
7. Yoshizawa S, Sugiyama KT, Mancini D, Marboe CC (2013) Characteristics of patients with advanced heart failure having eosinophilic infiltration of the myocardium in the recent era. *Int Heart J* 54(3):146–148
8. Yokoyama T, Miyazawa K, Kurakawa E, et al. (2004) Interstitial pneumonia induced by imatinib mesylate: pathologic study demonstrates alveolar destruction and fibrosis with eosinophilic infiltration. *Leukemia* 18(3):645–646
9. Del BM, Deck JH, Davidson GS (2000) Glial swelling with eosinophilia in human post-mortem brains: a change indicative of plasma extravasation. *Acta Neuropathol* 100(6):688–694
10. Yoo SY, Han JK, Kim YH, et al. (2003) Focal eosinophilic infiltration in the liver: radiologic findings and clinical course. *Abdom Imaging* 28(3):326–332
11. Kim YK, Kim CS, Moon WS, et al. (2005) MRI findings of focal eosinophilic liver diseases. *Am J Roentgenol* 184(5):1541–1548
12. Lee MH, Kim SH, Kim H, Lee MW, Lee WJ (2011) Differentiating focal eosinophilic infiltration from metastasis in the liver with gadoxetic acid-enhanced magnetic resonance imaging. *Korean J Radiol* 12(4):439–449
13. Sun JS, Kim JK, Won JH, et al. (2005) MR findings in eosinophilic infiltration of the liver. *J Comput Assist Tomogr* 29(2):191–194
14. Kim TH, Kim JK, Lee JH, et al. (2009) Focal eosinophilic infiltration versus metastasis in the liver: comparison of MRI findings. *Hepatogastroenterology* 56(94–95):1471–1476
15. Dellon ES, Aderoju A, Woosley JT, Sandler RS, Shaheen NJ (2007) Variability in diagnostic criteria for eosinophilic esophagitis: a systematic review. *Am J Gastroenterol* 102(10):2300–2313
16. Lee WJ, Lim HK, Lim JH, et al. (1999) Foci of eosinophil-related necrosis in the liver: imaging findings and correlation with eosinophilia. *Am J Roentgenol* 172(5):1255–1261
17. Schmiedl U, Paajanen H, Arakawa M, Rosenau W, Brasch RC (1988) MR imaging of liver abscesses; application of Gd-DTPA. *Magn Reson Imaging* 6(1):9–16
18. Lim JH, Lee WJ, Lee DH, Nam KJ (2000) Hypereosinophilic syndrome: CT findings in patients with hepatic lobar or segmental involvement. *Korean J Radiol* 1(2):98–103
19. Ogbogu PU, Bochner BS, Butterfield JH, et al. (2009) Hypereosinophilic syndrome: a multicenter, retrospective analysis of clinical characteristics and response to therapy. *J Allergy Clin Immunol* 124(6):1319–1325
20. Salkic NN, Mustedanagic-Mujanovic J, Jovanovic P, Alibegovic E (2013) Enhanced therapeutic response with addition of loratadine in subserosal eosinophilic gastroenteritis. *Med Glas (Zenica)* 10(1):178–182
21. Ahn SJ, Choi JY, Kim KA, et al. (2011) Focal eosinophilic infiltration of the liver: gadoxetic acid-enhanced magnetic resonance imaging and diffusion-weighted imaging. *J Comput Assist Tomogr* 35(1):81–85
22. Schlund JF, Semelka RC, Kettritz U, Eisenberg LB, Lee JK (1995) Transient increased segmental hepatic enhancement distal to portal vein obstruction on dynamic gadolinium-enhanced gradient echo MR images. *J Magn Reson Imaging* 5(4):375–377
23. Cha SH, Park CM, Cha IH, et al. (1998) Hepatic involvement in hypereosinophilic syndrome: value of portal venous phase imaging. *Abdom Imaging* 23(2):154–157